



THERMAL PROPERTIES OF ENHANCEMENT STUDY ON GAS TURBINE BLADES AFTER BARRIER COATINGS ON BLADE PROFILE

T. ANJANEYULU*1, K CHANDRA SEKHAR *2, Dr B. SUDHEER PREMKUMAR*3

1*. M. tech (Thermal) Student, Department of Mechanical Engineering, 1*QIS College of Engineering and Technology Ongole, Prakasam Dist, A.P – 523272

2*. Associate Professor, Department of Mechanical Engineering, 1*QIS College of Engineering and Technology Ongole, Prakasam Dist, A.P – 523272

3* Professor, Department of Mechanical Engineering, JNTUCEH, JNTU Hyderabad

Email: anji66as@gmail.com

Abstract:

Barrier coatings on gas turbine chambers are normally feasible in all the cases as an study barrier coats at high heat flux areas on the blade profiles also an important task the blade geometry playing critical role and the dimension tolerances will be less to machine exact coated dimension need to perform machining dimension for drawing preparation present study focused on the barrier coats with Ni and TiB₂ with different spray feeds and its layer thick ness has been studied by using SEM test for after coating now a days different materials for using for blade preparation with forging techniques the work performed on 3mm thickness plates with spray control methods by changing spraying temperatures the thickness of the coat will be varied to 0.05,0.075, and 0.1mm the thermal barrier coats restrict degradability in high temperature gas turbine blades.

Key words: barrier coats gas turbine blades, SEM coat thickness

1.0 INTRODUCTION

Gas turbines are used for aircraft propulsion and for terrestrial or industrial applications in the production of electricity. Increasing the thermal performance and power output of advanced gas turbines are main elements for the production of modern turbine cooling. Different key factors affect a gas turbine system's thermal efficiency or fuel consumption:

- Increase in the turbine inlet temperature, called firing temperature.
- Reduction of cooling air usage.
- Improving components efficiencies.
- Enhancement of cycle

The increase in turbine intake temperature is constrained by its metal-alloyed capability (fuel liners, valves and blades in practice) for the manufacture of turbine components. The component's working temperature is just below the material's melting point. The turbine input temperature represents the gas turbine power output.

Components of Steam Turbine:

The part of a steam turbine is mostly fixed in a single direction in the blades, the part of a blade is the very high temperature, which is absorbed by the blades and then the combustor produces the high-pressure turbine and its blades are compounded with very limited components.

The steam blade carrier condenses the steam turbine. In this case, we use the guides to guide the blades which are going to be fixed blades, in order to get some high work fluid at high order pressure.

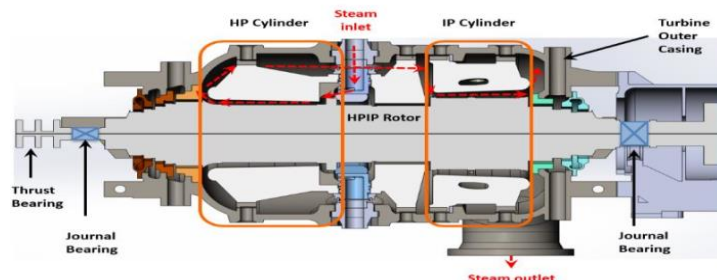


Figure: Components of Steam Turbine

Applications of Gas Turbine:

The following are the applications of gas turbine as shown in figure

- Central power stations,
- Industrial and Industrial.
- Space Applications:
- Turbo jet and Turbo prop.
- Marine application

Advantages of Gas Turbine

- Quite high ratio of power to weight in comparison to inverse engines.
- Smaller than most mutual motors with the same efficiency.
- Moves in one direction, with even less noise than a reciprocal engine.
- More moving elements than mutual motors.

Problem of the statement:

The problem is defined as the answer of blade stresses to the gas temperature and turbine speed variations. The problem is the problem. We conducted structural and thermal analysis using different gas temperatures and turbine speeds in this mission. We defined stresses on the blade and the temperature spread across the blade by doing the analysis above

Objectives

1. Enhance the protection of blades with heat-resistant and coating applications in high temperature gas turbine engines.
2. To estimate and analyse the performance of gas turbine using references to hot-blade coatings.
3. To evaluate blade efficiency with regard to thermal barrier content coatings and the effect of construction.

2.0 LITERATURE REVIEW

[1] Numerical work has been carried out on enhanced thermal transfer through the rectangular channel of turbulent flow which roughened by inclined ribs. The effects of turbulent flux and heat transfer were seen in the research in a channel fitted with inclined disconnected ribs, the number of Reynolds varied from 4 to 103 to 24 to 103.

[2] Presented an experimental and computational analysis to approximate heat transfer efficiency of different ribs. The rectangular ribbed channel friction loss and heat transfer efficiency, with a variety of rib configurations analyzed via 3D Reynolds equations were averaged by Naiver Stokes.

Dempsey, E et al [3] Many experiments have demonstrated the advantages of the use of gas turbine wave rotor systems. General trends in performance have been generated, but where the best design space is concerned is. The goal of the research is to respond to the query by showing widespread performance patterns in multi-dimensional areas in many four-port rotor tops.

Wellman, R. G et al [4] The addition of thermal barrier coatings to internal cooling components in the hot gas stream of gas turbine engines has helped steeply increase the entry temperature of the turbine and the resulting improved gas turbine engine output and capacity.

Duhua Wang et al [5] Sol – gel protective coatings exhibit excellent thermal stability, prevention of oxidation and increased resistance to corrosion of the metal substrates. The sol-gel solution is also a surface-resistant technique that shows the ability for removal of harmful pre-treatments and coatings, typically used to improve corrosion resistance in metals. This analysis deals with the production and uses of durable sol-gel coats, including steel, aluminium, copper and magnesium and their alloys for various metal substrates.

3.0 METHODOLOGY

Turbine Blade is an extraction tool that meets the maximum performance requirements of aerodynamics, construction and thermal. Over the last few decades, gas-turbine engine operating temperatures have increased to improve motor power and performance. More work into improved combustion temperatures Nickel-based super alloys operate at the internal cooling temperature around 1.300°C and $950 - 1175^{\circ}\text{C}$ without internal cooling has been performed to boost the efficiency of gas turbine engines for aircraft applications. Nickel is an

essential property of a Jet Motor that prevents corrosion and works to operate components. It is around 1 1728 K (1 455 ° C) at its melting point. It can shape alloys, which are a key aspect, in particular with aluminum as a compound known as gamma prime that maintain its resistance at high temperatures Nickel alloys maintain their strength almost as high as 85% of the melting point as Steel or Titanium, while 40-5% of the melting point is observed to decrease fastly. Nickel-based super alloys also work very well at high temperatures, a blessing for aviation.

BLADE DESIGN:

The new blade design improves aerodynamic blades close to the root of the blade and thereby reduces both the loss of the profile and the final wall. The new rotor blade was found to increase its efficiency by about 0.3 percent on the basis of the results of 3D phase- and air turbine tests.

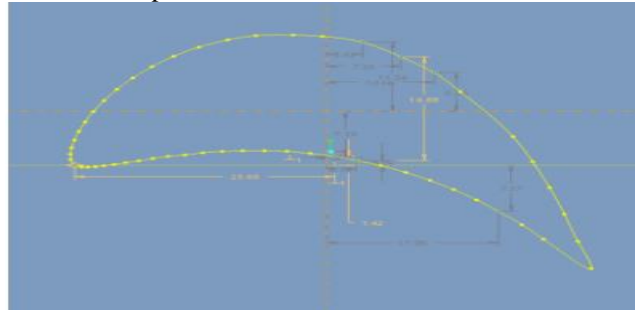


Figure: 3.1 Sketcher Profile of Blade

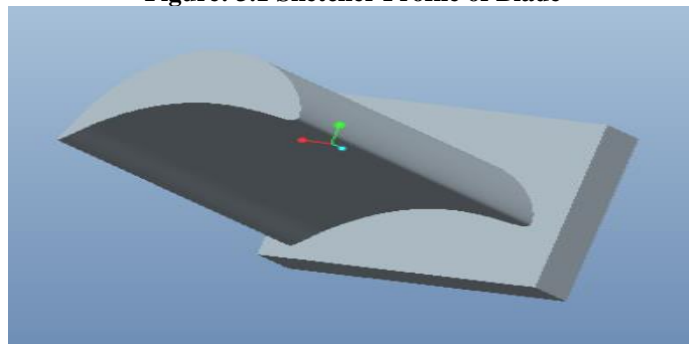


Figure: 3.2 Blade with Base

MATERIAL PROPERTIES:

The blade material should be a Creep strength, creep fatigue tolerance, Notch sensitivity and damping property, as we discussed in the literature survey under the subheading "Recommended material properties for gas turbine bladder." Chromium steel nickel alloy is one such substance that has all these characteristics

Blade speed N = 8000 rpm

Blade cross-sectional area A = 165.161 mm²

Material density ρ = 7850x10⁻⁶ kg/mm³

Blade tip radius r₂ = 267.5 mm

Blade root radius r₁ = 220.5 mm

Blade length r₂-r₁ = 47mm

Chromium steel:

Chromium steels are steel types in which iron may be chromium alloyed. Colloquially the term stainless steel also comes in interchangeable form. Chromium is not inherent in stainless steel in nature, but chrome is one of the most common alloys in stainless steel grades and is found in most commonly produced grades of stainless steel.

Properties:

- Atomic Symbol: Cr
- Atomic Number: 24
- Atomic Mass: 51.996g/mol¹
- Element Category: Transition Metal
- Density: 7.19g/cm³ at 20°C
- Melting Point: 3465°F (1907°C)
- Boiling Point: 4840°F (2671°C)
- Moh's Hardness: 5.5

Nickel alloy properties:

Nickel and nickel alloys are highly durable non-ferrous metals, good resistance to corroding and outstanding temperature properties. Alloy 625 is solid, nickel-chrome-cobalt-molybdenum alloy with an outstanding high-temperature mix strength and resistance to oxidation. The alloy also has an outstanding resilience against a vast number of corrosive conditions and is conveniently molded and welded using traditional methods.

Nickel Alloy 617 provides customers with a specific chemical composition which consists of:

- Ni 44.5%
- Cr 20-24%
- Co 10-15%
- Mo 8-10%
- Fe 3% max
- Si 1% max
- Al .8-1.5%
- Ti 0.6% max

Nickel Alloy 188:

188 is a cobalt based alloy which provides good oxidation resistance to 2000 ° F with excellent heat resistance. The alloy is also highly sulphidated, good metallurgical stability and good ductility, after prolonged exposure to high temperatures.

- Density 0.330 lb/in³ 9.14 g/cm³
- Melting Range 2375-2425 ° F 1300-1330 ° C
- Specific Heat 0.097 at 70 ° F, Btu/lb ° F 405 at 21 ° C, J/kg ° C
- Permeability 1.0007 at 200 oersted
- Coefficient of Expansion 6.6 0-200 ° F, 10⁻⁶ in/in

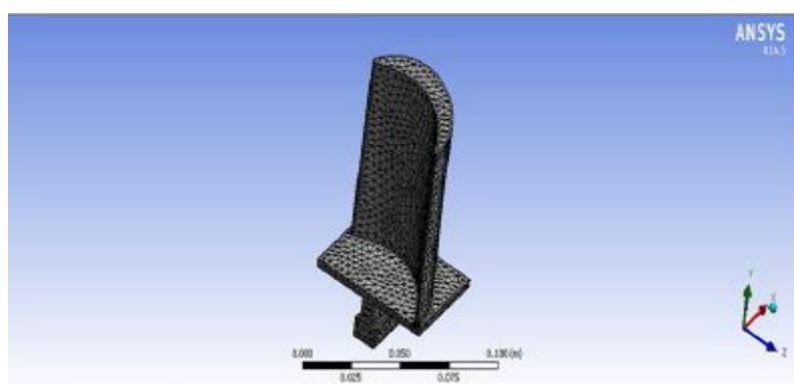


Figure: 3.3 Mashed model

The continuous thermal analysis shows that the temperatures and heat fluxes of the rotor blade of the gas turbine. The temperature distribution figure shows the copper material gas turbine rotor blade distribution. In this figure, the maximum temperature is observed at the front surface and at the trailing edge of the rotor blade the minimum temperature is observed.

4.0 RESULTS AND DISCUSSIONS

An individual portion that forms the turbine part of a gas turbine is a turbine blade. The blades extract energy from the high-temperature gas created by the combustion system. The turbine blades are often the small gas turbines part. Turbine blades also use unusual material, such as super alloys and various forms of colding, such as internal air channels, cooling lying boundary and thermal hazard coverings to survive in this challenging environment.

Thermal analysis of gas turbine blade:

Heat transfer coefficients of the bladder are analysed in order to determine the heat transfer rate. Chromium steel is the material used in the blade. It is superseded by Nickel alloys in this project. The better material is analysed for the blade.

4.2 Thermal analysis of blade materials:

CHROMIUM STEEL, NICKEL ALLOY 617 AND NICKEL ALLOY 188

MATERIAL PROPERTIES:

Chromium Steel Thermal conductivity = 24.38W/m-k

Nickel Alloy 617 Thermal conductivity = 13.6W/m-k

Nickel Alloy 188 Thermal conductivity = 24.1W/m-k

MATERIAL - CHROMIUM STEEL:

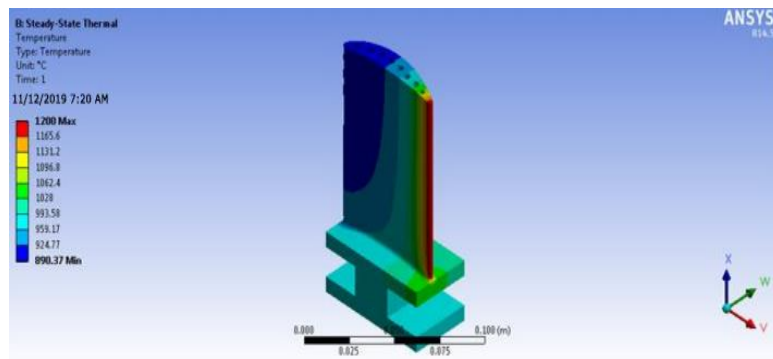


Figure: 4.1 Temperature distributions

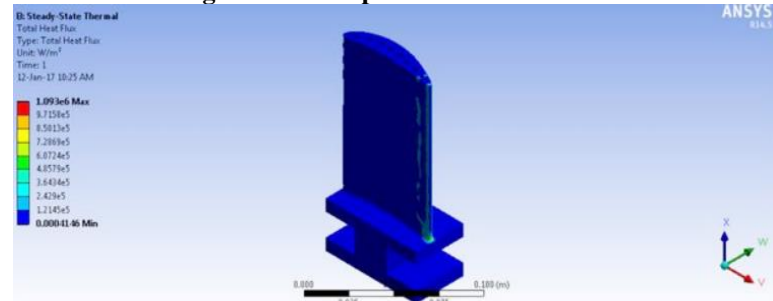


Figure: 4.2 heat flux

NICKEL ALLOY 617:

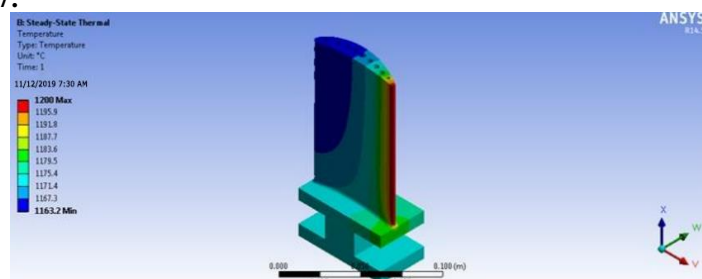


Figure: 4.3 Temperature distribution NICKEL ALLOY 617

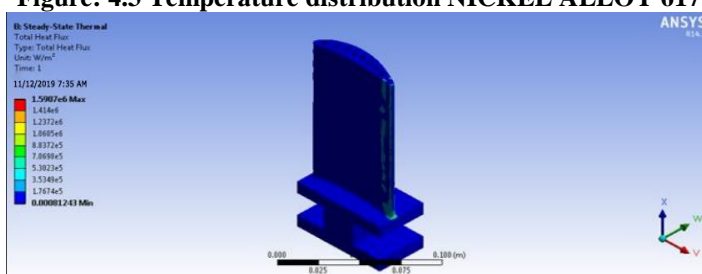


Figure: 4.4 heat flux NICKEL ALLOY 617

Nickel Alloy 188:

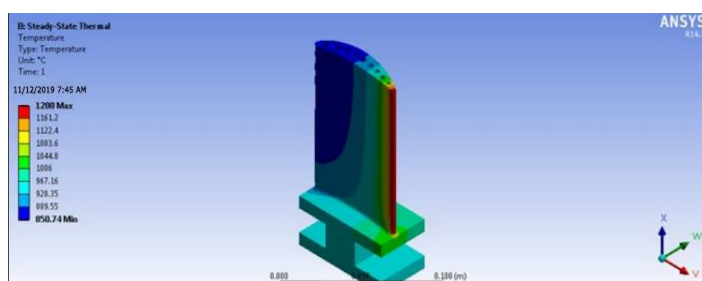


Figure: 4.5 Temperature distribution NICKEL ALLOY 188

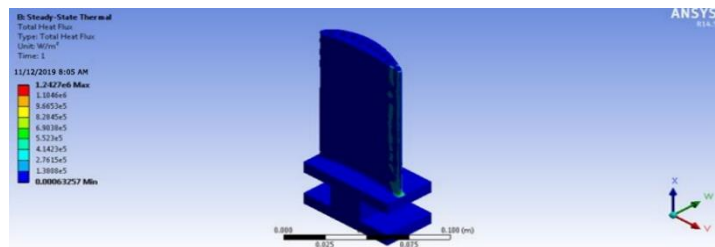
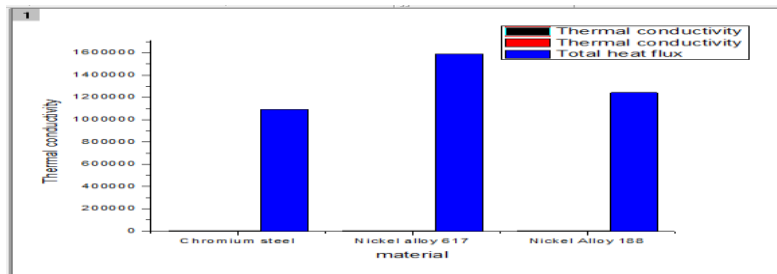


Figure: 4.6 heat flux NICKEL ALLOY 188

Table: 4.1 Thermal Analysis Results Of Gas turbine blade

Material	Thermal conductivity		Total heat flux
	Maximum	Minimum	
Chromium steel	1200	924.77	1.093e6
Inconel alloy 725	1200	1167.3	1.590e6
Inconel alloy 625	1200	899.5	1.2427e6



Graph: 4.1 Thermal Analysis

CFD ANALYSIS OF GAS TURBINE BLADE:

The distribution of temperature and total heat transfer rates depend on the heat transfer coefficient of the gas and the material's thermal conductance. Some iterative methods such as realizable (k-e) turbulence models can be used to calculate the heat transfer coefficient. The maximum temperatures at the leading edge of the blade are observed

Boundary condition:

Inlet velocity: 128 m/s

Temperature at inlet: 644 K

Pressure outlet : Gauge pressure

Fluid: air

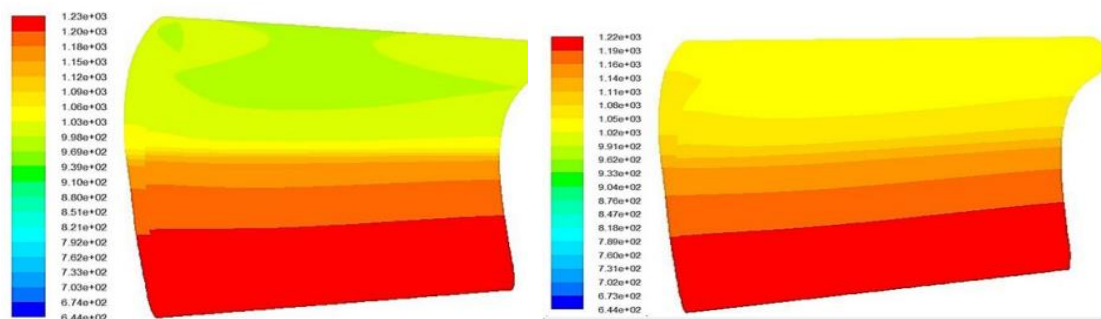


Figure: 4.7 Static temperature (K) contour of W = 0.3. and W = 0.25.

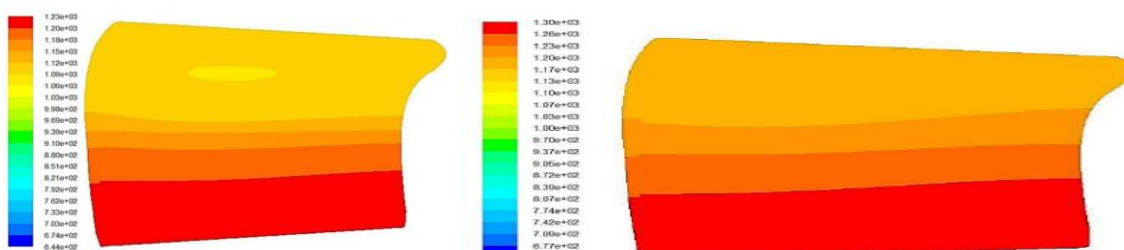


Figure: 4.8 Static temperature (K) Contour of W = 0.20. and W = 0.15.

Simulation of the gas turbine in the CFD program without positioning stacks on the trailing edge is carried out with twisted tape insert configurations for width ratio from $W + = 0,3$ until $W = 0,15$. Figure for $W = 0,3, 0,25, 0,2$ and $0,15$ shows a statically-tempered contour of $W = 0,3$ and provides a longer flow path for the water and therefore facilitates secondary diffusion production in comparison to certain widths a significant amount of heat transfer takes place. Nevertheless, the heat transfer rate increases as the distance ratio tends to decrease.

Experimental Procedure:

The blade composite was a cast Super-Metal Ni-Basis known as Inconel 738 LC with the mechanical characteristics given in the table. The tensile strengths of all components at the working temperature were measured during this analysis, owing to the relationship between the working temperature of the metal and the requirements of it. Compared to the thermal conditions at the height of this type of gas turbine engine, combustion materials have a temperature of around 560°C at the lead and 520°C at the rear edge of the engine and a turbine that has been running for approx. 73500 hours, causing significant losses to the turbine due to blade loss. Two adjacent were subjected to detailed failure examination in addition to the failed weapon. The following test series was carried out on the blades:

- Photographic and audio inspection evidence.
- Depth calculation of the cross section beneath the top of the fracture.
- Chemical bladder content research.
- A metallographic cross section analysis of the air foil and root blade sections as well as the analysis of the microprobe.
- Surface crack test using optical and electron microscopes

After coating blade:

Thermal barrier coatings (TBCs) are mounted on the turbine surface, decreasing the sub-substratum temperature and providing oxidation protection and heating from high-temperature gas corrosion. The barrier coats of various Ni- and TiB₂ sprays and their thickness layer is tested through the help of SEM for the use of various coating for the preparation of blades of blades, after a duration of several days, by adjusting the spray temperatures function on 3 mm spray control plates with different thicknesses would vary the coat's thickness between 0.05, 0.075 and 0.1 mm.

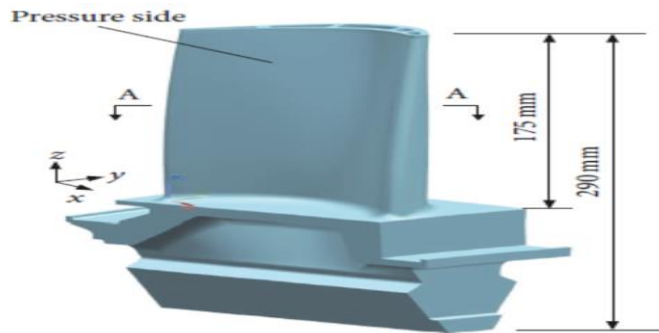


Figure: 4.9 Geometries of a gas turbine rotor blade after coating: (a) suction side view, (b) pressure side view, (c) internal cooling passages.

The blade is hollow and includes several cooling passages for the pressurized air. The root blade of the blade, which can attach it to the rotor disk, is not present in this model, as it has little impact on the problem. The feature of the air foil twists around the radial central line from the platform radially outwards to the blade's tip, as can be seen in Figure. Figure shows the dimension of a cross-section of the air foil.

Material Properties and Boundary Conditions:

TBCs consist of the substratum TiB₂ and nickel superalloy. All layers are considered isotropic, homogeneous and independent of the temperature. Table A uniform temperature limits were imposed on the blade without taking thermal radiation and convection into account, the properties of the steel.

Table: 4.2 Materials properties used in the finite element model

Material properties	Top-coat	TGO	Bond-coat	Substrate
Elasticity modulus (GPa)	48.0	400	200	220
Poisson's ratio	0.1	0.23	0.3	0.31
Thermal expansion coefficient ($\times 10^{-6}/^{\circ}\text{C}^{-1}$)	9.0	8.0	13.6	12.6
Thermal conductivity (W/m ² °C)	1.2	10.0	5.8	11.5

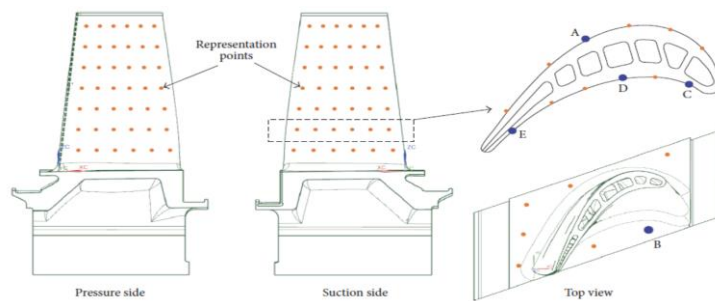


Figure: 4.10 Distribution of the representative positions on the blade

The TC thickness is consistent throughout the entire coating region when the uniform thickness scheme is applied. Figure (taking as an example a 3-mm Uniform thickness scheme) The high temperature region on the substratum is generally located at the air film root, in particular at the platform of the blade the temperature of the substrate that is much lower than the front edge due to its slender and efficient intra-substrate cooling. Overall, the FE analyses show that the temperature on the air film of the substrate is significantly reduced when the TC thickness increases, but the platform is not evident.

TiB₂ Coating of turbine blade results:

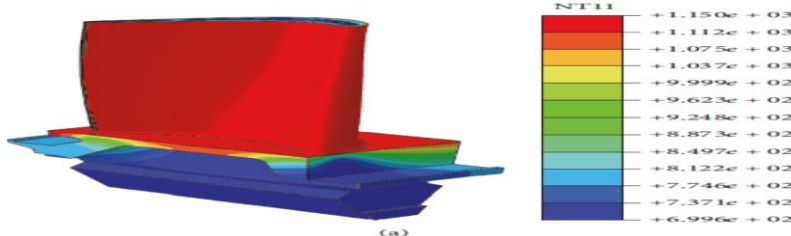


Figure: 4.11 uniform top-coat thickness 0.005 mm

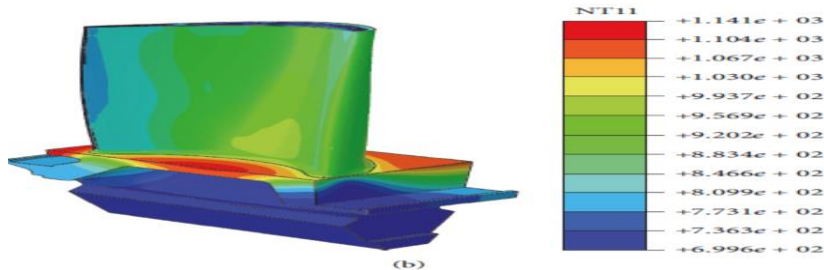


Figure:4.12 uniform top-coat thickness 0.075 mm

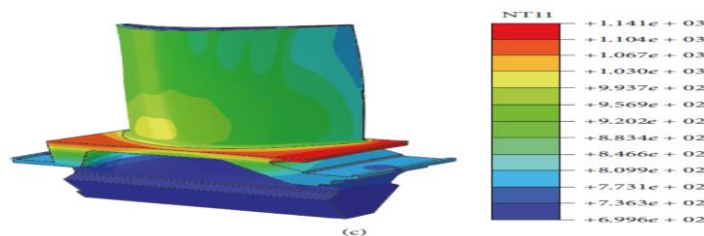


Figure: 4.13 uniform top-coat thickness 0.1 mm

We suggested three design schemes according to the preliminary findings and then compared these to find a suitable distribution of TC thickness. In general, the design of the distribution of layer thickness should take into account the realistic spraying process. The spinning feature of the air foil makes it possible to spray the coverings in the vertical direction by splitting the subregions.

Ni material coating results:

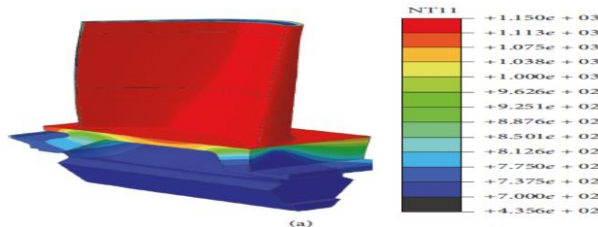


Figure: 4.14 uniform top-coat thickness 0.05 mm

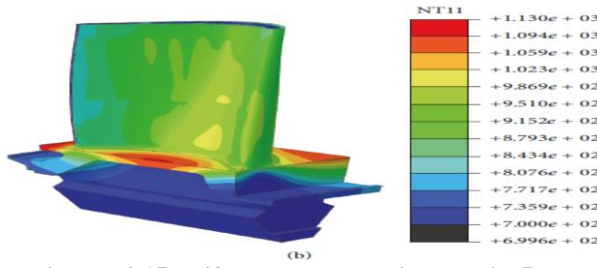


Figure: 4.15 uniform top-coat thickness 0.75 mm

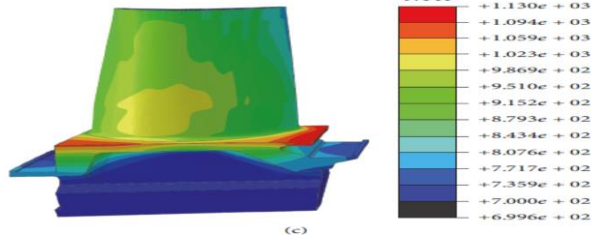


Figure: 4.16 uniform top-coat thickness 0.1 mm

For the distribution of thickness of sufficient thermal barrier covering (TBCs) for a real gas turbine fan. Three-dimensional TBC turbine blade finite element model was developed and evaluated and the weighted-sum approach was used to solve the multi-target optimization problem. In order to increase the performance of the coatings, the construction approach includes the objective comparative indicator of TBCs thickness.

SEM RESULTS:



Figure: 4.17 General view of the blade number 3 showing corroded regions. (a) Concave surface. (b) Convex surface.

Chromium steel with NI 0.05 mm coating:

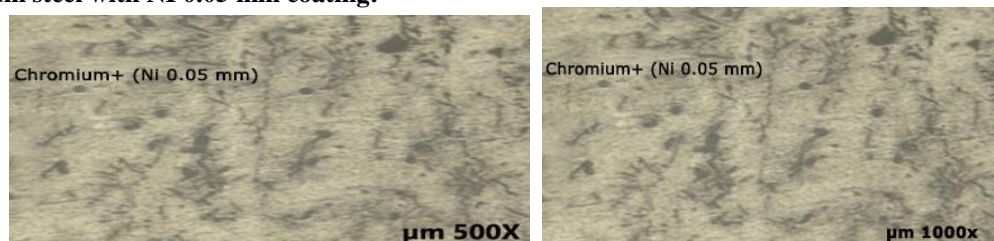


Figure: 4.18 Chromium steel with NI 0.05 mm coating 500x and 1000x

CHROMIUM STEEL WITH NI 0.075 MM COATING:

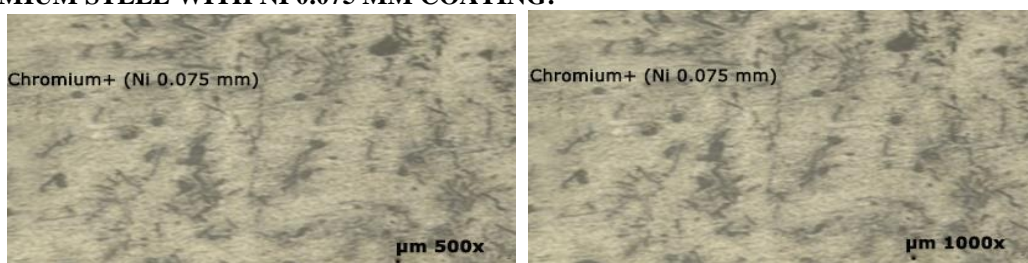


Figure: 4.19 Chromium steel with NI 0.075 mm coating 500x and 1000x

Chromium Steel with Ni 0.1 mm Coating

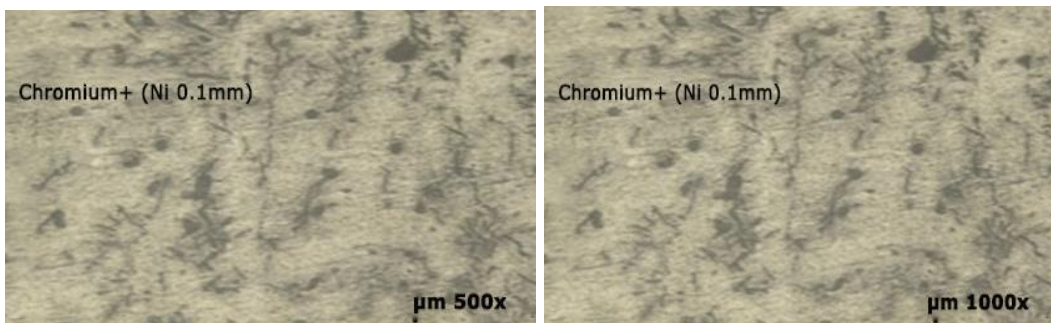


Figure: 4.20 Chromium steel with NI 0.1 mm coating 500x and 1000x
INCONEL ALLOY 725 MICRO STRUCTURAL ANALYSIS DIFFERENT THICKNESS
INCONEL WITH NI 0.05 mm COATING

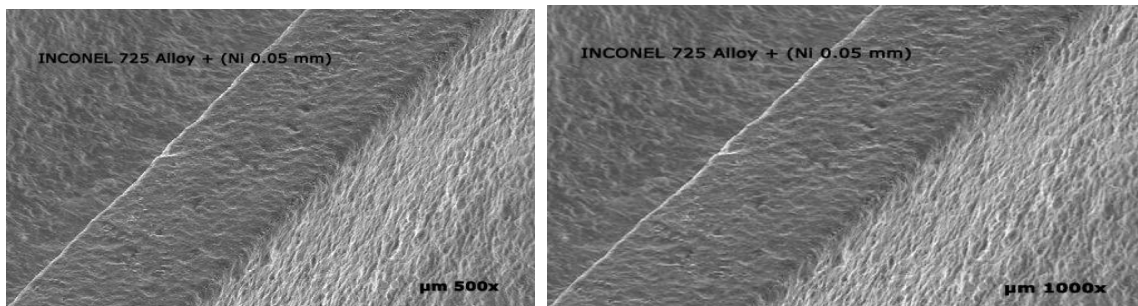


Figure: 4.21 Inconel725 with NI 0.05mm coating 500x and 1000x
INCONEL725 WITH NI 0.075mm COATING

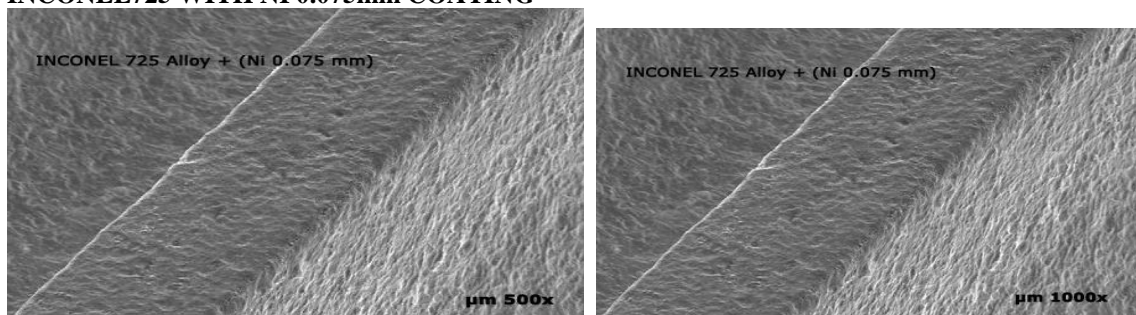


Figure:4.22 Inconel725 with NI 0.075mm coating 500x and 1000x
INCONEL 725 with Ni 0.1 mm Coating

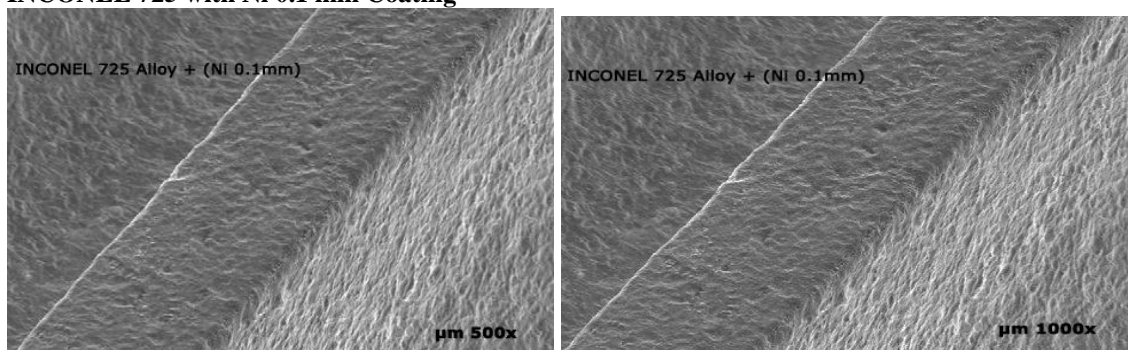


Figure: 4.23 Inconel725 with NI 0.1mm coating 500x and 1000x

INCONEL ALLOY 625 with 0.05mm coating

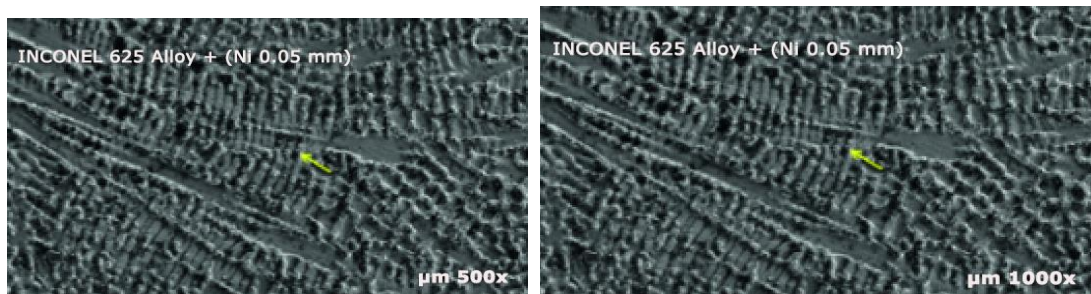


Figure: 4.24 Inconel 625 with NI 0.05mm coating 500x and 1000x
INCONEL ALLOY 625 with 0.75 mm coating

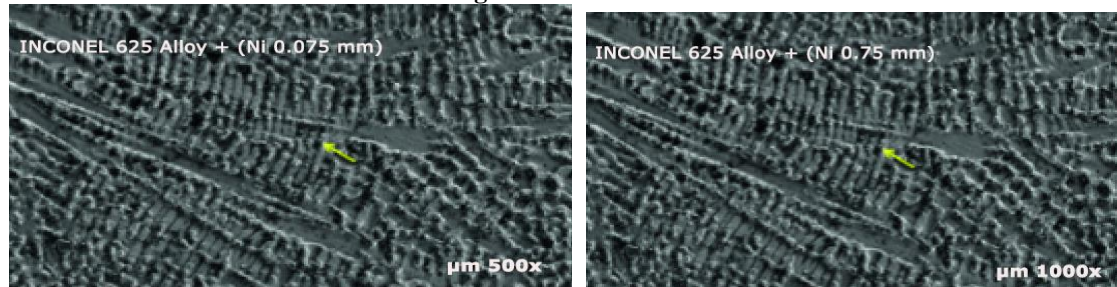


Figure: 4.25 Inconel 625 with NI 0.075 mm coating 1000x
INCONEL 625 with Ni 0.1 mm Coating

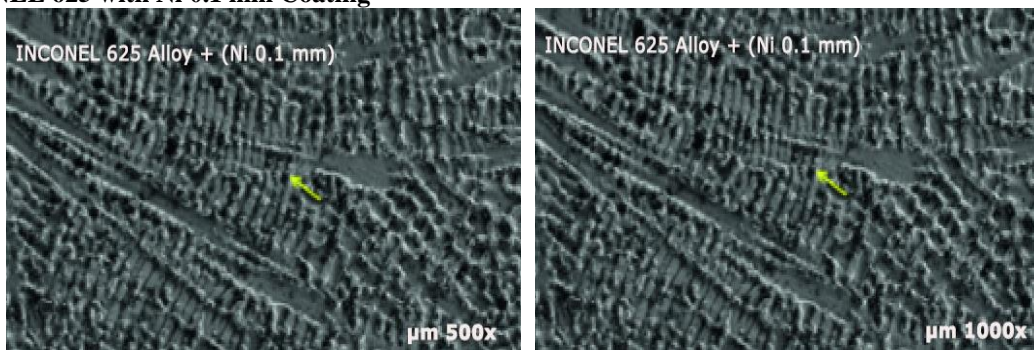


Figure: 4.26 Inconel 625 with NI 0.1 mm coating 500x and 1000x
CHROMIUM MATERIAL TiB₂ COATING
CHROMIUM MATERIAL TiB₂ 0.1 MM COATING

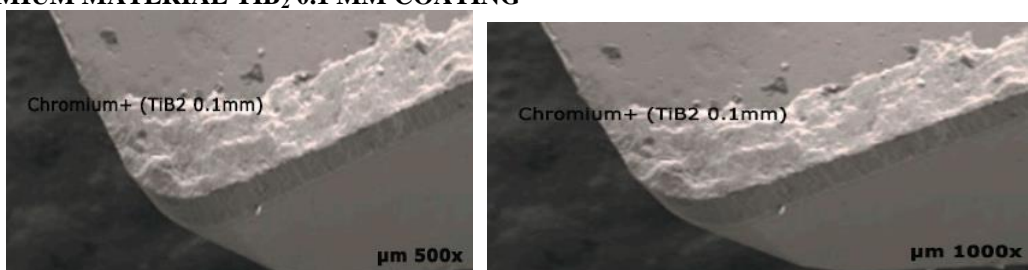


Figure: 4.27 Chromium material TiB₂ 0.1 mm coating 500X,1000X

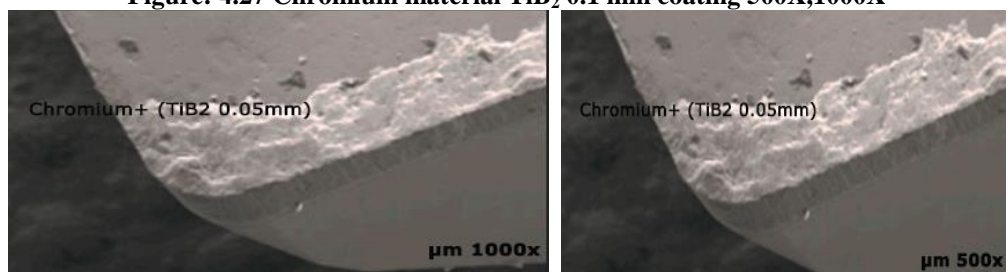
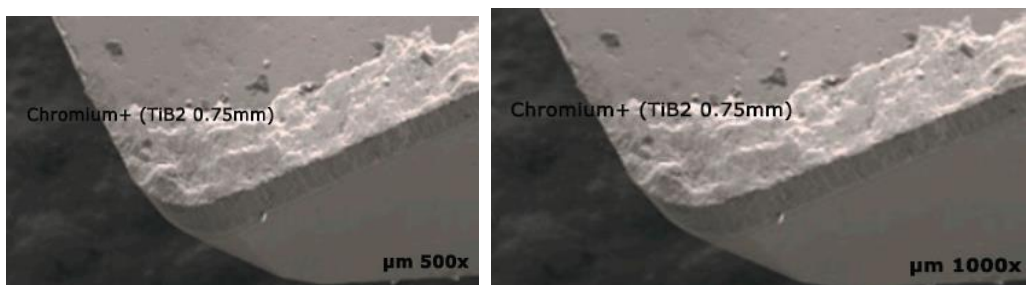
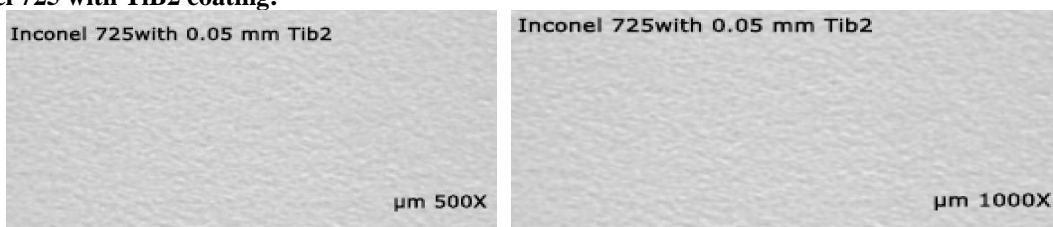
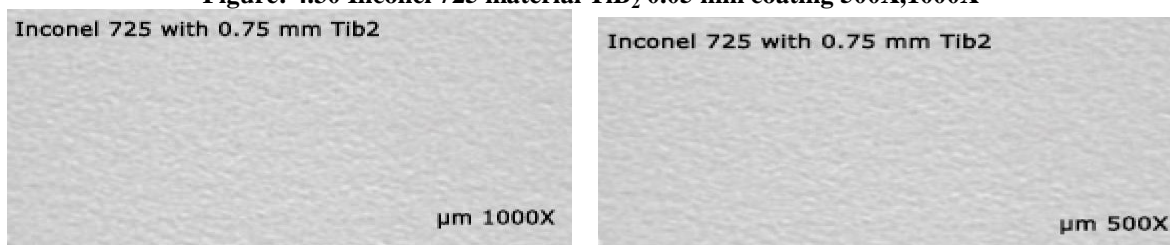
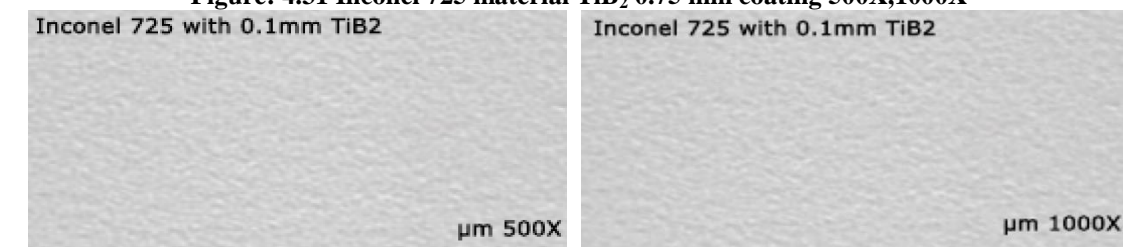
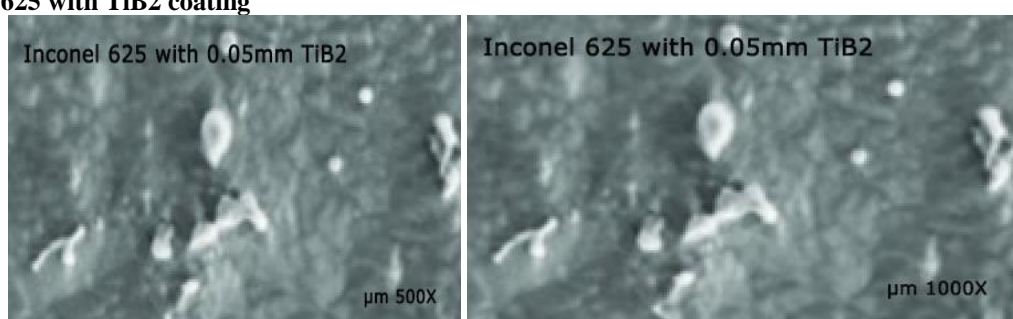
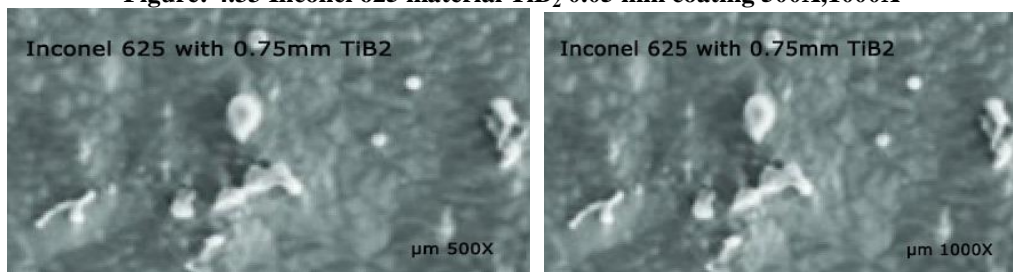


Figure: 4.28 Chromium material TiB₂ 0.05 mm coating 500X,1000X

Figure: 4.29 Chromium material TiB_2 0.75 mm coating 500X,1000XInconel 725 with TiB_2 coating:Figure: 4.30 Inconel 725 material TiB_2 0.05 mm coating 500X,1000XFigure: 4.31 Inconel 725 material TiB_2 0.75 mm coating 500X,1000XFigure: 4.32 Inconel 725 material TiB_2 0.1 mm coating 500X,1000XInconel 625 with TiB_2 coatingFigure: 4.33 Inconel 625 material TiB_2 0.05 mm coating 500X,1000XFigure: 4.34 Inconel 625 material TiB_2 0.75 mm coating 500X,1000X

Copyright @ 2020 ijearst. All rights reserved.

INTERNATIONAL JOURNAL OF ENGINEERING IN ADVANCED RESEARCH
SCIENCE AND TECHNOLOGY

Volume.02, IssueNo.11, November -2020, Pages: 248-261

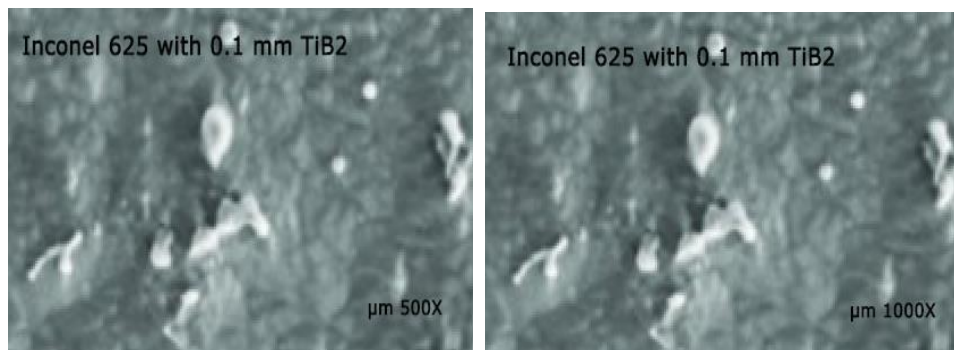
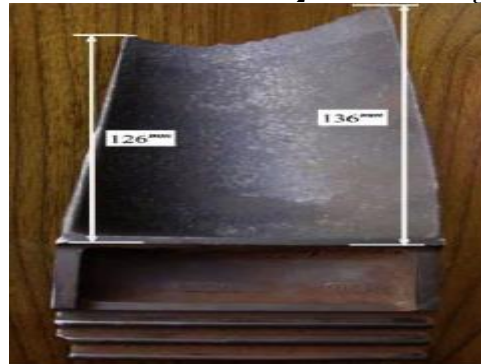
Figure: 4.35 Inconel 625 material TiB₂ 0.1 mm coating 500X,1000X

Figure: 4.36 The distance of the fracture surface from the platform at blade edges.

Chemical Analysis:

A bulk analysis was conducted by an Optics Emission Analyzer, ARC-MET 930 S&P, to determine the chemical composition of the blade fiber. The findings of chemical analysis show that the material is compatible with nickel alloy

X-RAY DIFFRACTION TECHNIQUE:

Micro-structure characterisation has also been carried out over many years, using X-ray diffraction (XRD) techniques. XRD can be used to determine the percentages of different phases of the specimen if the structures of the specimen are different. In the event of a particular phase being chemically removed from a large specimen, XRD based on the crystal structure and lattice dimensions can be identified. The energy spectrometer (EDS) analysis, when quantifying the chemical composition, can supplement this work.

CUTTING:

A sample is removed from the field examined. The sample size will be microscopically accurate. This analysis is based on a sample cut of 6mmx6 mm. Faster cuttings such as flame cutting, laser cutting, machining of electron discharging and so on are favoured for hands skiing, abrasive clipping, chemical and electrical-chemical cutting.

MOUNTING:

It is typically more practical to install it onto a resin for very small or irregularly formed specimens. The common use of bakelite. There are also multiple specimens that can be assembled from a single part and polished simultaneously. Don't mount various metals on the same table.



Figure: 4.37 Turbine blade specimens mounted in Bakelite

Gas turbine engine Its blades have been made of superalloy with nickel-based finishing to maintain high temperature and other environmental conditions. A microstructural evaluation of the blade material from 3 different areas (root, midspan and tip) of the blade reveals that due to operation of blades with high temperatures there were no microstructural harm, which indicates that the blades are operated in the designed / normal operating condition. Finally, it was decided that the turbine blade failure of a gas turbine for marine application decreased the fatigue strength of the blade which ultimately caused the failure of the turbine blades due to

multiple fault mechanisms such as hot corrosion, erosion and tiredness. The heat corrosion reduced the blade's thickness and thus weakened the edge.

CONCLUSION

By observing the results of thermal analyses, Inconel and Chromium Steel have almost the same heat flux. Thus, as Inconel 625,725 and Chromium Aluminium, heat transfer rates are higher. The strength of the nickel alloy 188, however, is greater than the force of Chromium Steel. Tests show a stronger cooling effect than the other when using turbine-blade insert ($W=0.3$) for distance. The blade temperature is reduced by about 34 per cent on the front edge, ie from 1561 K to approx. by the use of twisted tape inserts $W = 0.3$ (without stack). This indicates that the turbine pales essentially cool down from 1030 K and about 21 percent on the trailing line, i.e. from 1561 K up to around 1230 K. While efficient refrigeration of the turbine blades can increase their service life, it can also reduce the engine's thermal performance. In addition, the coating surface temperature was reduced by performing a transpiration cooling test, simulating the field of gas stream around the gas turbine blades, and the cooling hole dropped concentrically around the cooling hole. This showed the efficacy of the transpiration cooling system in tandem with the porous ceramic coating for the gas turbine rim.

REFERENCES:

1. T. Sadowski, P. Golewski "Multidisciplinary analysis of the operational temperature increase of turbine blades in combustion engines by application of the ceramic thermal barrier coatings (TBC)". elsevier Computational Materials Science 50, 2011, pp:1326-1335.
2. M. Gell, D. N. Duhl, D. K. Gupta and K. D. Sheffler, "Advanced superalloy airfoils," Journal of Metals, 1987, pp:11-15.
3. Biao Li, Xueling Fan, Dingjun Li and Peng Jiang."Design of thermal barrier coatings thickness for gas turbine blade based on finite element analysis". Mathematical Problems in Engineering Volume 2017, Article ID 2147830,2017,13 pages.
4. Theju V , Uday P S , PLV Gopinath Reddy , C.J.Manjunath. "Design and analysis of gas turbine blade". International Journal of Innovative Research in Science, Engineering and Technology. Vol. 3, Issue 6, June 2014 pp:13533-13539.
5. W. Zhu, J.W. Wang , L. Yang, Y.C. Zhou , Y.G. Wei, R.T. Wu. "Modeling and simulation of the temperature and stress fields in a 3D turbine blade coated with thermal barrier coatings".elsevier Surface and coatings technology 315,2017,pp:443-453.
6. X.Q. Cao, R. Vassen, D. Stoever. "Ceramic materials for thermal barrier coatings". elsevier, Journal of the European Ceramic Society 24, 2004,pp:1–10.
7. Ebi A. Ogirikia Yiguang G. Li "Effect of fouling, thermal barrier coating degradation and film cooling holes blockage on gas turbine engine creep life" elsevier The Fourth International Conference on Through-life Engineering Services ,2015,pp: 228 – 233.
8. Robert Vaßen , Maria Ophelia Jarligo, Tanja Steinke, Daniel Emil Mack, Detlev Stöver "Overview on advanced thermal barrier coatings" Elsevier Surface & Coatings Technology 205,2010, pp: 938–942